

This is the accepted manuscript made available via CHORUS. The article has been published as:

Theory of many-body radiative heat transfer without the constraint of reciprocity

Linxiao Zhu, Yu Guo, and Shanhui Fan

Phys. Rev. B **97**, 094302 — Published 7 March 2018

DOI: [10.1103/PhysRevB.97.094302](https://doi.org/10.1103/PhysRevB.97.094302)

Theory of many-body radiative heat transfer without the constraint of reciprocity

Linxiao Zhu,^{*} Yu Guo, and Shanhui Fan[†]

*Department of Electrical Engineering, Ginzton Laboratory,
Stanford University, Stanford, California 94305, USA*

Abstract

Using a self-consistent scattered field approach based on fluctuational electrodynamics, we develop compact formulas for radiative heat transfer in many-body systems without the constraint of reciprocity. The formulas allow for efficient numerical calculation for a system consisting of a large number of bodies, and are in principle exact. As a demonstration, for a non-reciprocal many-body system, we investigate persistent heat current at thermal equilibrium and directional heat transfer when the system is away from thermal equilibrium.

I. INTRODUCTION

It has been theoretically shown^{1–5} and experimentally verified^{6–17} that near field radiative heat transfer between bodies supporting surface waves can greatly exceed the blackbody limit. These results indicate the fundamental importance for the study of thermal electromagnetic fluctuation at nanoscale, and may lead to opportunities for applications such as imaging^{18,19}, thermo-photovoltaics^{20–26}, electroluminescent cooling^{27,28}, thermal rectifier^{29–34} and thermal transistor³⁵.

Near-field radiative heat transfer is strongly geometry-dependent. A variety of photonic structures such as gratings^{36–47}, metamaterials^{48–51}, thin films^{11,52,53} have been used to tailor near field radiative heat transfer. Therefore, there are significant efforts in developing the theoretical formalisms to treat near-field heat transfer in various geometries^{1–5,35,54–62}. The vast majority of these works have focused on heat transfer between two bodies. Moreover, the electromagnetic properties of these bodies are typically assumed to be reciprocal, where the permittivity and permeability are described by scalars or symmetric tensors⁶³.

On the other hand, it has been recently noted that new physics effects can arise when one considers many-body heat transfer^{35,58}. Also, for heat transfer between non-reciprocal bodies, novel effects, such as a thermal Hall effect⁶⁴, or a persistent heat current at equilibrium⁶⁵, can arise. These effects, moreover, exist only in systems consisting of at least three bodies. More specifically, for two bodies 1 and 2 in a many-body system, we denote the spectral heat transfer to body 2 due to thermal noise sources in body 1 as $S_{1\rightarrow 2}(\omega)$, and the spectral heat transfer to body 1 due to thermal noise sources in body 2 as $S_{2\rightarrow 1}(\omega)$. If such many-body system consists of materials that violate Lorentz reciprocity, when bodies 1 and 2 have the same temperature, the radiative heat transfer between bodies 1 and 2 are non-reciprocal, i.e. $S_{1\rightarrow 2}(\omega) \neq S_{2\rightarrow 1}(\omega)$. In light of these recent developments, there is therefore a need for developing a theoretical formalism that treats many-body heat transfer without the constraint of reciprocity.

In this paper, we develop compact formulas for radiative heat transfer in both reciprocal and non-reciprocal arbitrarily-shaped many-body systems. Our development uses a self-consistent scattered field approach within the framework of fluctuational electrodynamics, and are in principle exact. The formulas can be used for efficient numerical calculation for a system containing a large number of bodies, without any constraint on whether the

electromagnetic response of these bodies are reciprocal or not. As a demonstration, we show that the effect of persistent equilibrium heat current, which was previously observed in a system consisting of three non-reciprocal bodies⁶⁵, also exists as one further increases the number of bodies. Moreover, such a heat current has signatures in non-equilibrium situations. Our work should prove useful in exploring new opportunities of controlling near field radiative heat transfer by using complex non-reciprocal or reciprocal many-body systems.

Related to our works, there have been several other efforts in developing a theory for many-body heat transfer. And here we briefly contrast our works with these efforts. A formalism for reciprocal many-body heat transfer was provided in Ref. 57. But the formalism requires knowing beforehand the collective scattering effect (i.e. the T-matrix) for a composite consisting of multiple bodies. Obtaining the T-matrix of a composite containing a large number of bodies is non-trivial and therefore it requires substantial further work in order to directly implement the formalism of Ref. 57 to compute many-body heat transfer. In contrast, in this article, we describe the many-body heat transfer in terms of the scattering effect (i.e. the T-matrix) of *individual* objects. We show that our formula can be efficiently implemented numerically. We also note that non-reciprocal heat transfer in a three-body system is studied in Ref. 65 using a scattering approach, but Ref. 65 does not allow treating many-body systems consisting of a large number of bodies. Our formalism also differs from the dipole approximation approach^{64,66–69} for many-body heat transfer in that our approach takes into account all the modes. The dipole approximation is most accurate when the particles are smaller than the thermal wavelength, and the spacing between the particles is relatively large as compared to the size of the particles. Our formalism is not restricted to this regime and can be used to treat situations where higher order modes may contribute significantly to the radiative heat transfer. Finally, we note that a thermal discrete dipole approximation (T-DDA) method has been used to study radiative heat transfer between magneto-optical materials⁶¹. In T-DDA, each body needs to be discretized into a large number of volume elements and hence requires one to solve linear systems with a large number of unknowns. In contrast, the use of a scattering method such as ours typically results in linear systems with a far smaller number of unknowns and thus is much faster than methods that require spatial discretization⁷⁰. The relatively modest computational costs of our scattering approach further allow for studying many-body radiative heat transfer in a

system consisting of a large number of bodies.

The rest of the paper is organized as follows. In Section II we discuss the mathematical background. In Section III we summarize the main results. In Section IV we derive formulas for many-body radiative heat transfer for an arbitrary number of bodies without the constraint of reciprocity. In Section V, based on the formulas we derived in Section IV, we study non-reciprocal many-body radiative heat transfer at both equilibrium and non-equilibrium situations. We conclude in Section VI.

II. MATHEMATICAL BACKGROUND

A. Assumptions

We start by briefly summarizing the assumptions that underlie our approach. We consider a many-body system that consists of linear materials. Our approach applies independent of whether the materials satisfy Lorentz reciprocity or not.

The multiple bodies in the system may have different temperatures. We assume that the temperature inside each body is homogeneous. We note that in certain scenarios there may be non-negligible temperature inhomogeneity even in nanoscale bodies. In particular, a volumetric-fluctuating current formalism has been used to study effects of temperature inhomogeneity on radiative heat transfer and thermal radiation^{71,72}. We do not consider such inhomogeneity in our approach even though our approach may be generalized for such situations.

We use a scattering formalism and expand fields using a complete basis. Specifically, in order to use the spherical wave basis as the complete basis, the bodies can have arbitrary shapes, however, each body must be able to be enclosed by non-overlapping spheres.

B. Notation

Throughout the paper we use the SI units and the $e^{-i\omega t}$ convention. All time-dependent physical fields, e.g. $A(t)$ are real. The convention for Fourier transform is

$$A(t) = \text{Re} \int_0^\infty d\omega A(\omega) e^{-i\omega t}. \quad (1)$$

For thermal calculation, the relevant physical quantities are typically in the form of $\langle A(t)B(t) \rangle$, where $\langle \dots \rangle$ denotes an ensemble average. The thermal processes we consider in the paper are stationary random processes, where $\langle A(t)B(t) \rangle$ is time-independent. Therefore $\langle A(\omega)B^*(\omega') \rangle$ must be proportional to $\delta(\omega - \omega')$, i.e.

$$\langle A(\omega)B^*(\omega') \rangle = \langle AB^* \rangle_\omega \delta(\omega - \omega'). \quad (2)$$

Using Eqs. 1 and 2, we have

$$\langle A(t)B(t) \rangle = \int_0^\infty d\omega \frac{1}{2} \text{Re} \langle AB^* \rangle_\omega.$$

In particular, the Poynting vector

$$\mathbf{S} = \langle \mathbf{E}(t) \times \mathbf{H}(t) \rangle = \int_0^\infty d\omega S(\omega) \equiv \int_0^\infty d\omega \frac{1}{2} \text{Re} \langle \mathbf{E} \times \mathbf{H}^* \rangle_\omega,$$

where \mathbf{E} and \mathbf{H} are electric and magnetic fields, respectively.

C. Electromagnetic scattering theory

We briefly summarize the relevant aspect of the electromagnetic scattering theory, and highlight those aspects unique to non-reciprocal systems. Assuming a permittivity and permeability distribution $\epsilon(\mathbf{r})$, $\mu(\mathbf{r})$, in the presence of an electric current source \mathbf{J} at a frequency ω , the resulting electric field \mathbf{E} satisfies

$$(\hat{H}_0 - \hat{V} - \frac{\omega^2}{c^2} \hat{I}) \mathbf{E} = i\omega\mu_0 \mathbf{J}, \quad (3)$$

where

$$\begin{aligned} \hat{H}_0 &= \nabla \times \nabla \times, \\ \hat{V} &= \frac{\omega^2}{c^2} (\hat{\epsilon} - \hat{I}) + \nabla \times (\hat{I} - \frac{1}{\hat{\mu}}) \nabla \times. \end{aligned}$$

Here μ_0 is the permeability of vacuum. $\hat{\epsilon}$ and $\hat{\mu}$ are the operator forms for $\epsilon(\mathbf{r})$ and $\mu(\mathbf{r})$. Eq. 3 can be formally solved as

$$\mathbf{E} = i\omega\mu_0 \hat{G} \mathbf{J},$$

where

$$\hat{G} = \left(\hat{H}_0 - \hat{V} - \frac{\omega^2}{c^2} \hat{I} - i\eta \right)^{-1}, \quad (4)$$

is the Green function operator. Here η is an infinitesimal positive number. We denote the free-space Green's function as \hat{G}_0 . \hat{G}_0 is symmetric, i.e. $\hat{G}_0(\mathbf{r}, \mathbf{r}') = \hat{G}_0^T(\mathbf{r}', \mathbf{r})$.

Consider a body surrounded by vacuum. In the presence of an incident wave in vacuum \mathbf{E}_0 , the resulting total field \mathbf{E} satisfies the Lippmann-Schwinger equation⁷³

$$\mathbf{E} = \mathbf{E}_0 + \hat{G}_0 \hat{V} \mathbf{E}. \quad (5)$$

Define the \hat{T} operator such that $\hat{T}\mathbf{E}_0 = \hat{V}\mathbf{E}$, we then have also

$$\mathbf{E} = \mathbf{E}_0 + \hat{G}_0 \hat{T} \mathbf{E}_0. \quad (6)$$

The scattering property of the body is therefore entirely described by the \hat{T} operator. Using Eqs. 5 and 6, the \hat{T} operator can be solved as:

$$\hat{T} = \hat{V}(\hat{I} - \hat{G}_0 \hat{V})^{-1}. \quad (7)$$

For most previous works in near-field heat transfer, both ϵ and μ are assumed to be either scalar or symmetric tensors, in which cases the system satisfies Lorentz reciprocity. And from Eqs. 4 and 7, both \hat{G} and \hat{T} are symmetric, i.e. $\hat{G}(\mathbf{r}, \mathbf{r}') = \hat{G}^T(\mathbf{r}', \mathbf{r})$, and $\hat{T}(\mathbf{r}, \mathbf{r}') = \hat{T}^T(\mathbf{r}', \mathbf{r})$. On the other hand, in this paper we will be considering systems without reciprocity constraint. In these systems ϵ and μ may no longer be symmetric, such as in magneto-optical materials as we will simulate in Section V. For these systems, in general \hat{G} and \hat{T} are not symmetric operators.

In this paper we make extensive use of various solutions of the free-space Maxwell's equations, which can be written as:

$$(\hat{H}_0 - \frac{\omega^2}{c^2} \hat{I}) \mathbf{E} = 0. \quad (8)$$

The set of non-singular solutions of this equation for all frequencies, which we denote as \mathbf{E}_ν^{reg} , form a complete basis, with ν denoting the labels. In the spherical coordinate system, for example, $\nu \equiv \{l, m, P\}$, where l , m and P are the total angular momentum, and the angular momentum component along the z -direction, and the polarization index, respectively. We also denote the solutions of this equation, with an outgoing-wave boundary condition, as \mathbf{E}_ν^{out} . In the spherical or cylindrical coordinate system centered around an origin, the outgoing waves are singular at the origin.

For arbitrary wave basis, the regular and outgoing wave basis functions satisfy the following orthonormal relations:

$$-Im \oint [\mathbf{E}_\nu^{out} \times (\nabla \times \mathbf{E}_{\nu'}^{out*}) g + \mathbf{E}_{\nu'}^{out} \times (\nabla \times \mathbf{E}_\nu^{out*}) g^*] \cdot d\mathbf{A} = 2Re(g) \delta_{\nu\nu'} \delta_{\nu,pr}, \quad (9)$$

$$-Im \oint [\mathbf{E}_\nu^{out} \times (\nabla \times \mathbf{E}_{\nu'}^{reg*}) g + \mathbf{E}_{\nu'}^{reg} \times (\nabla \times \mathbf{E}_\nu^{out*}) g^*] \cdot d\mathbf{A} = Re(e^{-i\phi_\nu} g) \delta_{\nu\nu'}, \quad (10)$$

$$-Im \oint [\mathbf{E}_\nu^{reg} \times (\nabla \times \mathbf{E}_{\nu'}^{reg*}) g + \mathbf{E}_{\nu'}^{reg} \times (\nabla \times \mathbf{E}_\nu^{reg*}) g^*] \cdot d\mathbf{A} = 0, \quad (11)$$

where g is an arbitrary complex number. Here, the integration is taken on a closed surface surrounding the origin, and $d\mathbf{A}$ denotes outward-pointing surface area element. In Eq. 9, $\delta_{\nu,pr} = 1$ for a basis function ν that is propagating, and is zero otherwise. In Eq. 10, ϕ_ν is zero for propagating basis function, and is generally a non-zero real number for evanescent basis function. Identities equivalent to Eqs. 9, 10 and 11 in cylindrical wave basis for the subset of propagating basis functions were used in Ref. 74.

Spherical wave basis only consists of propagating waves. Thus, in spherical wave basis, Eqs. 9 and 10 simplify to

$$-Im \oint [\mathbf{E}_\nu^{out} \times (\nabla \times \mathbf{E}_{\nu'}^{out*}) g + \mathbf{E}_{\nu'}^{out} \times (\nabla \times \mathbf{E}_\nu^{out*}) g^*] \cdot d\mathbf{A} = 2Re(g) \delta_{\nu\nu'}, \quad (12)$$

$$-Im \oint [\mathbf{E}_\nu^{out} \times (\nabla \times \mathbf{E}_{\nu'}^{reg*}) g + \mathbf{E}_{\nu'}^{reg} \times (\nabla \times \mathbf{E}_\nu^{out*}) g^*] \cdot d\mathbf{A} = Re(g) \delta_{\nu\nu'}. \quad (13)$$

The free-space Green's function can be expanded using outgoing and regular wave basis functions:

$$\hat{G}_0(\mathbf{r}, \mathbf{r}') = i \sum_{\nu} \mathbf{E}_\nu^{out}(\mathbf{r}) \otimes \mathbf{E}_{\sigma(\nu)}^{reg}(\mathbf{r}'), \quad (14)$$

when $|\mathbf{r}| > |\mathbf{r}'|$. We note that Eq. 14 is the representation of the free-space Green's function in scattering wave basis, while Eq. 4 is the general Green function operator. Here, $\sigma(\nu)$ denotes a permutation of the mode index ν . $\sigma(\{l, m, P\}) = \{l, -m, P\}$ for the spherical wave basis function. We note that Eq. 14 is “on-shell”: for the free-space Green's function at a frequency ω , the right hand side of Eq. 14 involves only the solutions of Eq. 8 at the frequency ω . The imaginary part of the free-space Green's function can be expanded using propagating regular wave basis functions:

$$Im \hat{G}_0(\mathbf{r}, \mathbf{r}') = \sum_{\nu \in pr} \mathbf{E}_\nu^{reg}(\mathbf{r}) \otimes \mathbf{E}_{\sigma(\nu)}^{reg}(\mathbf{r}'), \quad (15)$$

where again the right hand side involves solutions only at the frequency ω .

In arbitrary wave basis, the matrix element for the \hat{T} operator of a scatterer is defined as⁵⁷:

$$\mathcal{T}_{\nu\nu'} = i \int d\mathbf{r} \int d\mathbf{r}' \left[\mathbf{E}_{\sigma(\nu)}^{reg}(\mathbf{r}) \right]^T \hat{T}(\mathbf{r}, \mathbf{r}') \mathbf{E}_{\nu'}^{reg}(\mathbf{r}'). \quad (16)$$

D. Fluctuation dissipation theorem

Thermal radiation is sourced by fluctuating current sources. For a medium without magnetic loss (i.e. $\hat{\mu} = \hat{\mu}^\dagger$), at a temperature T , the current-current correlation function has the form

$$\langle \mathbf{J}(\omega, \mathbf{r}) \mathbf{J}^\dagger(\omega', \mathbf{r}') \rangle = \frac{4}{\pi} \omega \Theta(\omega, T) \epsilon_0 \delta(\mathbf{r} - \mathbf{r}') \frac{\hat{\epsilon}(\mathbf{r}, \omega) - \hat{\epsilon}^\dagger(\mathbf{r}, \omega)}{2i} \delta(\omega - \omega'), \quad (17)$$

where $\Theta(\omega, T) = \hbar\omega / \left[\exp(\frac{\hbar\omega}{k_B T}) - 1 \right]$. This form is applicable to both reciprocal and non-reciprocal media^{75,76}.

For a system that is at equilibrium, e.g. a many-body system where all bodies are at the same temperature, the electric field correlation function has the form $\langle \mathbf{E}(\mathbf{r}, \omega) \mathbf{E}^\dagger(\mathbf{r}', \omega') \rangle = \delta(\omega - \omega') \langle \mathbf{E}(\mathbf{r}) \mathbf{E}^\dagger(\mathbf{r}') \rangle_\omega$, where

$$\langle \mathbf{E}(\mathbf{r}) \mathbf{E}^\dagger(\mathbf{r}') \rangle_\omega = \frac{4}{\pi} \omega \Theta(\omega, T) \mu_0 \frac{\hat{G}(\mathbf{r}, \mathbf{r}') - \hat{G}^\dagger(\mathbf{r}', \mathbf{r})}{2i}. \quad (18)$$

This can be seen as a manifestation of the fluctuation dissipation theorem⁷⁷, since the Green's function is the linear response function of the electromagnetic system with respect to \mathbf{J} . Alternatively, this relation can also be derived using Eqs. 4 and 17.

III. SUMMARY OF MAIN RESULTS

Having reviewed the mathematical background in the previous section, in this section we summarize the main results of the paper regarding the major properties of heat transfer in many-body systems without the constraint of reciprocity. We also contrast these properties with those in reciprocal systems. We consider a many-body system including n bodies, as schematically shown in Fig. 1. These bodies may have different temperatures. Without loss of generality we specifically discuss radiative heat transfer between bodies 1 and 2 in the many-body system. Using scattering theory, in this article, we will show that the spectral

heat flux to body 2 due to thermal noise sources in body 1, which is maintained at a temperature T_1 , can be expressed as

$$S_{1 \rightarrow 2}(\omega) = \frac{2}{\pi} \Theta(\omega, T_1) \text{Tr} \left[\mathcal{A}_2 \overline{\mathcal{W}}_{21} \mathcal{R}_1 \overline{\mathcal{W}}_{21}^\dagger \right], \quad (19)$$

where

$$\mathcal{A}_j = -(e^{-i\Phi_j} \mathcal{T}_j + \mathcal{T}_j^\dagger e^{i\Phi_j})/2 - \mathcal{T}_j^\dagger \Pi^{pr} \mathcal{T}_j \quad (20)$$

is related to the absorption process of the j -th body,

$$\mathcal{R}_j = -(\mathcal{T}_j e^{-i\Phi_j} + e^{i\Phi_j} \mathcal{T}_j^\dagger)/2 - \mathcal{T}_j \Pi^{pr} \mathcal{T}_j^\dagger \quad (21)$$

is related to the emission process of the j -th body. Here, \mathcal{T}_j is the T -matrix of the j -th body and is related to its scattering matrix \mathcal{S}_j by $\mathcal{T}_j = (\mathcal{S}_j - \mathcal{I})/2$ where \mathcal{I} is identity matrix. Π^{pr} is an operator that projects to the sub-space of propagating waves. Φ_j is a diagonal matrix. Its diagonal element is zero for propagating waves, and non-zero for evanescent waves. In Eq. 19, $\overline{\mathcal{W}}_{21}$ describes the scattering of outgoing waves from body 1 into regular waves impinging on body 2, taking into account of the scattering by all bodies in the many-body system. Generally, $\overline{\mathcal{W}}_{jk}$ is the (j, k) -th block element of $\overline{\mathcal{W}} \equiv \overline{\mathcal{U}}(\mathcal{I} - \overline{\mathcal{T}} \overline{\mathcal{U}})^{-1}$, where

$$\overline{\mathcal{T}} \equiv \begin{bmatrix} \mathcal{T}_1 & 0 & \dots & 0 \\ 0 & \mathcal{T}_2 & \dots & \dots \\ \dots & \dots & \dots & 0 \\ 0 & \dots & 0 & \mathcal{T}_n \end{bmatrix}, \quad \overline{\mathcal{U}} \equiv \begin{bmatrix} 0 & \mathcal{U}^{12} & \dots & \mathcal{U}^{1n} \\ \mathcal{U}^{21} & 0 & \dots & \dots \\ \dots & \dots & \dots & \mathcal{U}^{(n-1)n} \\ \mathcal{U}^{n1} & \dots & \mathcal{U}^{n(n-1)} & 0 \end{bmatrix}.$$

Here, \mathcal{U}^{jk} represents the translation matrix connecting the wave basis for body j and k .

Also, the emission from the source body 1 to the environment in the presence of other bodies is

$$S_{1 \rightarrow env}(\omega) = \frac{2}{\pi} \Theta(\omega, T_1) \text{Re} \sum_{j=1}^n \text{Tr} \left[\overline{\mathcal{Q}}_{j1} \mathcal{R}_1 (\Pi^{pr} \overline{\mathcal{Q}}_{j1} + e^{i\Phi_j} \overline{\mathcal{W}}_{j1})^\dagger \right]. \quad (22)$$

In Eq. 22, $\overline{\mathcal{Q}}_{jk}$ is the (j, k) -th block element of $\overline{\mathcal{Q}} \equiv (\mathcal{I} - \overline{\mathcal{T}} \overline{\mathcal{U}})^{-1}$.

The results above are for an arbitrary scattering wave basis. In a spherical wave basis, all basis functions are propagating waves. We have

$$\mathcal{A}_j = -(\mathcal{T}_j + \mathcal{T}_j^\dagger)/2 - \mathcal{T}_j^\dagger \mathcal{T}_j, \quad (23)$$

$$\mathcal{R}_j = -(\mathcal{T}_j + \mathcal{T}_j^\dagger)/2 - \mathcal{T}_j \mathcal{T}_j^\dagger. \quad (24)$$

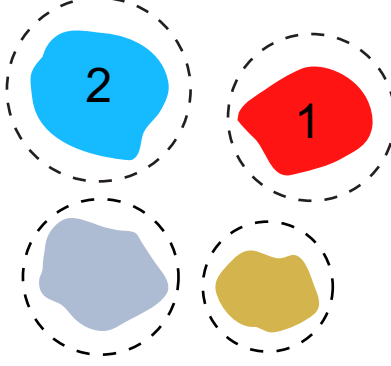


FIG. 1. (Color online) Schematic of a system consisting of multiple bodies in electromagnetic heat transfer with each other. For this specific case, spherical wave basis can be used, as the bodies can be surrounded by non-overlapping spheres.

The properties for \mathcal{A} and \mathcal{R} strongly depend on whether the system is reciprocal or not. In a system consisting only of materials satisfying Lorentz reciprocity, the \hat{T} operator is symmetric, hence by the definition of \mathcal{T} matrix in Eq. 16, we have $\mathcal{T}_{\nu\nu'} = \mathcal{T}_{\sigma(\nu')\sigma(\nu)}$. It follows that, for a reciprocal system, $\mathcal{A}_{\nu\nu'} = \mathcal{R}_{\sigma(\nu')\sigma(\nu)}$. Also, for a reciprocal system, one has $\mathcal{W}_{21,\nu\nu'} = \mathcal{W}_{12,\sigma(\nu')\sigma(\nu)}$. Then by using Eq. 19, it is straightforward to show that the radiative heat transfer between bodies 1 and 2 is reciprocal, i.e. $\mathcal{S}_{1\rightarrow 2}(\omega) = \mathcal{S}_{2\rightarrow 1}(\omega)$, when bodies 1 and 2 have the same temperature $T_1 = T_2$.

In contrast, in a system consisting of materials that break Lorentz reciprocity, \hat{T} is generally non-symmetric. And hence in general $\mathcal{A}_{\nu\nu'} \neq \mathcal{R}_{\sigma(\nu')\sigma(\nu)}$. The breaking of Lorentz reciprocity also leads to $\mathcal{W}_{21,\nu\nu'} \neq \mathcal{W}_{12,\sigma(\nu')\sigma(\nu)}$. It follows that the radiative heat transfer is generally no-longer reciprocal, i.e. $\mathcal{S}_{1\rightarrow 2}(\omega) \neq \mathcal{S}_{2\rightarrow 1}(\omega)$, even when bodies 1 and 2 are at the same temperature. Since any pair of bodies in the many-body system can be selected as bodies 1 and 2, the arguments here apply to any pair of bodies in a many-body system. In summary, for a non-reciprocal system, the absorption and emission processes can no longer be directly related, leading to non-reciprocal radiative heat transfer.

Non-reciprocal heat transfer does not violate the second law of thermodynamics. At thermal equilibrium, the net heat flux into each body remains zero. When all the bodies and the environment have the same temperature T , if we denote $S_{i\rightarrow j}(\omega) \equiv \frac{\Theta(\omega,T)}{2\pi} F_{i\rightarrow j}(\omega)$, $S_{i\rightarrow env}(\omega) \equiv \frac{\Theta(\omega,T)}{2\pi} F_{i\rightarrow env}(\omega)$, and $S_{env\rightarrow i}(\omega) \equiv \frac{\Theta(\omega,T)}{2\pi} F_{env\rightarrow i}(\omega)$, energy conservation requires

that the total heat flux into body j must be balanced by the total heat flux out of body j :

$$\begin{aligned} & \sum_{i \neq j} \int d\omega \frac{\Theta(\omega, T)}{2\pi} F_{i \rightarrow j}(\omega) + \int d\omega \frac{\Theta(\omega, T)}{2\pi} F_{env \rightarrow j}(\omega) \\ &= \sum_{i \neq j} \int d\omega \frac{\Theta(\omega, T)}{2\pi} F_{j \rightarrow i}(\omega) + \int d\omega \frac{\Theta(\omega, T)}{2\pi} F_{j \rightarrow env}(\omega), \end{aligned} \quad (25)$$

where the subscript *env* denotes the environment. For linear systems which does not involve frequency conversion, Eq. 25 leads to

$$\sum_{i \neq j} F_{i \rightarrow j}(\omega) + F_{env \rightarrow j}(\omega) = \sum_{i \neq j} F_{j \rightarrow i}(\omega) + F_{j \rightarrow env}(\omega). \quad (26)$$

IV. FORMALISM FOR NON-RECIPROCAL MANY-BODY RADIATIVE HEAT TRANSFER

A. Spherical basis

We now provide a derivation of the main results as discussed in Section III, by introducing a formulation for calculating near field radiative heat transfer in non-reciprocal many-body systems. For simplicity, we consider the spherical scattering wave basis first, and the modification from using an arbitrary scattering wave basis is discussed later in Section IV B. We consider a many-body system consisting of n bodies in radiative exchange with each other, labeled as body 1, 2, ... n , respectively. In order to use the spherical wave basis, the bodies can have arbitrary shapes, however, each body must be able to be enclosed by non-overlapping spheres as illustrated in Fig. 1. We refer to such a sphere that encloses only the j -th body as the j -th sphere.

Consider first a body k by itself, i.e. in the absence of all other bodies. Suppose further that body k is in local thermal equilibrium of temperature T_k . Using Eq. 18, Lippmann-Schwinger equations^{57,73} and expansion on the scattering wave basis^{57,78}, we have (see Appendix for a derivation)

$$\langle \mathbf{E}(\mathbf{r}) \mathbf{E}^\dagger(\mathbf{r}') \rangle_{k, \omega}^{iso} = \frac{4}{\pi} \omega \Theta(\omega, T) \mu_0 \sum_{\nu, \nu'} \mathbf{E}_{k, \nu}^{out}(\mathbf{r}) (\mathcal{R}_k)_{\nu, \nu'} \mathbf{E}_{k, \nu'}^{out\dagger}(\mathbf{r}'), \quad (27)$$

where

$$\mathcal{R}_k = -(\mathcal{T}_k + \mathcal{T}_k^\dagger)/2 - \mathcal{T}_k \mathcal{T}_k^\dagger. \quad (28)$$

Here, \mathcal{T}_k denotes the T -matrix for body k , and $\mathbf{E}_{k,\nu}^{out}$ denotes the ν -th normalized outgoing wave basis function with respect to body k . For subsequent use we also use $\mathbf{E}_{k,\nu}^{reg}$ to denote the ν -th normalized regular wave basis function with respect to body k . Eq. 27 describes correlations of the emitted fields sourced by fluctuations in the k -th body only. We can also expand the field emitted by the isolated k -th body, \mathbf{E}^{iso} , in terms of the outgoing wave basis function with respect to the k -th body as:

$$\mathbf{E}^{iso} = \sum_{\nu} d_{k,\nu}^0 \mathbf{E}_{k,\nu}^{out}, \quad (29)$$

where $d_{k,\nu}^0$ is the expansion coefficient. From Eqs. 27 and 29, we have

$$\langle d_k^0 d_k^{0\dagger} \rangle = \frac{4}{\pi} \omega \Theta(\omega, T) \mu_0 \mathcal{R}_k, \quad (30)$$

where d_k^0 denotes a column vector of the coefficients $d_{k,\nu}^0$.

In the many-body system, the emitted fields sourced by body k as described by Eqs. 27 and 29 will be scattered by all the other bodies in the system. In order to evaluate the heat transfer from body k to body j , we need to calculate the field on body j that results from the thermal noise sources in body k , taking into account the scattering from all the bodies.

In the presence of the emitted field from the k -th body, the total field \mathbf{E} in the many body system in the free space regions outside all the bodies can be expanded in the outgoing wave basis defined with respect to all the individual bodies, i.e.

$$\mathbf{E} = \sum_{\nu, m} d_{mk,\nu} \mathbf{E}_{m,\nu}^{out}, \quad (31)$$

where $d_{mk,\nu}$ denotes the expansion coefficient.

Consider first the field in the free-space region that is outside the j -th body, but lies in the j -th sphere that encloses only the j -th body. In this region, we can rewrite Eq. 31 as:

$$\mathbf{E} = \sum_{\nu} d_{jk,\nu} \mathbf{E}_{j,\nu}^{out} + \sum_{\nu, m \neq j} d_{mk,\nu} \mathbf{E}_{m,\nu}^{out}. \quad (32)$$

In the case where $j \neq k$, we can interpret the second term in Eq. 32 as the wave that is incident on the j -th body, and the first term as the scattered wave by the j -th body in response to such incident wave. Therefore, we can derive a relation between these two terms by applying the Lippmann-Schwinger formalism⁷³ to the field inside the j -th sphere. We define an incident field that exists in the entire j -th sphere

$$\mathbf{E}_0 = \sum_{\nu, m \neq j} d_{mk,\nu} \mathbf{E}_{m,\nu}^{out}. \quad (33)$$

Inside the j -th sphere, such incident field can be expanded in the regular wave basis with respect to the j -th body:

$$\mathbf{E}_0 = \sum_{\nu} c_{jk,\nu} \mathbf{E}_{j,\nu}^{reg}, \quad (34)$$

where $c_{jk,\nu}$ is the expansion coefficient. In this region, outgoing wave basis functions with respect to the m -th body where $m \neq j$ can be expanded using regular wave basis functions with respect to the j -th body^{79,80}:

$$\mathbf{E}_{m,\nu}^{out} = \sum_{\nu'} \mathcal{U}_{\nu'\nu}^{jm} \mathbf{E}_{j,\nu'}^{reg}, \quad (35)$$

where \mathcal{U}^{jm} represents the translation matrix. From Eqs. 33 and 35, we have

$$\mathbf{E}_0 = \sum_{m \neq j, \nu} \mathbf{E}_{j,\nu}^{reg} \left(\sum_{\nu'} \mathcal{U}_{\nu'\nu}^{jm} d_{mk,\nu'} \right). \quad (36)$$

Then by comparing Eq. 36 with Eq. 34, we have

$$c_{jk} \equiv \sum_{m \neq j} \mathcal{U}^{jm} d_{mk}. \quad (37)$$

By applying the Lippmann-Schwinger equation⁷³ to calculate the field in the region that is inside the j -th sphere but outside the j -th body, we then have

$$\mathbf{E} = \mathbf{E}_0 + \hat{G}_0 \hat{T}_j \mathbf{E}_0. \quad (38)$$

From Eq. 34 and the relation $\hat{G}_0 \hat{T}_j \mathbf{E}_{j,\nu}^{reg} \equiv \sum_{\nu'} \mathbf{E}_{j,\nu'}^{out} \mathcal{T}_{j,\nu'\nu}$, we have

$$\mathbf{E} = \sum_{\nu} c_{jk,\nu} \mathbf{E}_{j,\nu}^{reg} + \sum_{\nu'} \mathbf{E}_{j,\nu'}^{out} \sum_{\nu} \mathcal{T}_{j,\nu'\nu} c_{jk,\nu}. \quad (39)$$

Then by comparing Eqs. 32 and 39, we have

$$d_{jk,\nu} = d_{jk,\nu}^{scat} \equiv \sum_{\nu'} \mathcal{T}_{j,\nu\nu'} c_{jk,\nu'}. \quad (40)$$

In the case where $j = k$, the field in the region that is inside the k -th sphere but outside the k -th body can also be written in the form of Eq. 32. The outgoing wave however, has contributions both from the source inside the k -th body, and from the scattering of the incident waves as represented by the first term, i.e.

$$d_{kk,\nu} = d_{k,\nu}^0 + d_{kk,\nu}^{scat}, \quad (41)$$

where the scattering part can be derived in the same wave as above. Eqs. 40 and 41 can be grouped as:

$$d_{jk} = \delta_{jk} d_k^0 + \mathcal{T}_j c_{jk}, \quad (42)$$

where δ_{jk} is the Kronecker delta function.

Eqs. 37 and 42 describe a full set of self-consistent equations. Plugging Eq. 37 into Eq. 42, we have

$$\begin{bmatrix} d_{1k} \\ \vdots \\ d_{kk} \\ \vdots \\ d_{nk} \end{bmatrix} = (\mathcal{I} - \overline{\mathcal{T}} \overline{\mathcal{U}})^{-1} \begin{bmatrix} 0 \\ \vdots \\ d_k^0 \\ \vdots \\ 0 \end{bmatrix} \quad (43)$$

for $k = 1, \dots, n$, with

$$\overline{\mathcal{T}} \equiv \begin{bmatrix} \mathcal{T}_1 & 0 & \dots & 0 \\ 0 & \mathcal{T}_2 & \dots & \dots \\ \dots & \dots & \dots & 0 \\ 0 & \dots & 0 & \mathcal{T}_n \end{bmatrix}, \quad \overline{\mathcal{U}} \equiv \begin{bmatrix} 0 & \mathcal{U}^{12} & \dots & \mathcal{U}^{1n} \\ \mathcal{U}^{21} & 0 & \dots & \dots \\ \dots & \dots & \dots & \mathcal{U}^{(n-1)n} \\ \mathcal{U}^{n1} & \dots & \mathcal{U}^{n(n-1)} & 0 \end{bmatrix}.$$

Thus, the (j, k) -th block element of $\overline{\mathcal{Q}} \equiv (\mathcal{I} - \overline{\mathcal{T}} \overline{\mathcal{U}})^{-1}$, which we denote as $\overline{\mathcal{Q}}_{jk}$, describes the relation between the outgoing waves from body j and the emitted outgoing waves from the isolated body k , i.e. $d_{jk} = \overline{\mathcal{Q}}_{jk} d_k^0$. Also, from Eqs. 37 and 43, we have

$$\begin{bmatrix} c_{1k} \\ \vdots \\ c_{kk} \\ \vdots \\ c_{nk} \end{bmatrix} = \overline{\mathcal{U}} \begin{bmatrix} d_{1k} \\ \vdots \\ d_{kk} \\ \vdots \\ d_{nk} \end{bmatrix} = \overline{\mathcal{U}} (\mathcal{I} - \overline{\mathcal{T}} \overline{\mathcal{U}})^{-1} \begin{bmatrix} 0 \\ \vdots \\ d_k^0 \\ \vdots \\ 0 \end{bmatrix}. \quad (44)$$

Thus, the (j, k) -th block element of $\overline{\mathcal{W}} \equiv \overline{\mathcal{U}} (\mathcal{I} - \overline{\mathcal{T}} \overline{\mathcal{U}})^{-1}$, which we denote as $\overline{\mathcal{W}}_{jk}$, describes the relation between the regular waves on body j and the emitted outgoing waves from the isolated body k , i.e. $c_{jk} = \overline{\mathcal{W}}_{jk} d_k^0$.

Based on the computation above, in the presence of all the other bodies, the resulting field, in the j -th sphere outside the j -th body, can be written as:

$$\mathbf{E} = \sum_{\nu} [d_{jk,\nu} \mathbf{E}_{j,\nu}^{out} + c_{jk,\nu} \mathbf{E}_{j,\nu}^{reg}]. \quad (45)$$

The heat flux into body j is

$$S_j = \int_0^\infty S_j(\omega) d\omega, \quad (46)$$

where $S_j(\omega) = -\oint d\mathbf{A} \cdot \frac{1}{2} \text{Re} \langle \mathbf{E} \times \mathbf{H}^* \rangle_\omega$, with the integration taken on the surface of the j -th sphere. Using Eqs. 45, 30, as well as the orthonormal relations of the regular and outgoing waves in Eqs. 11, 12 and 13, we obtain:

$$S_j(\omega) = -\frac{2}{\pi} \Theta(\omega, T_k) \text{Tr} \text{Re} [\overline{\mathcal{Q}}_{jk} \mathcal{R}_k (\overline{\mathcal{Q}}_{jk} + \overline{\mathcal{W}}_{jk})^\dagger], \quad (47)$$

where $j = 1, 2, \dots, n$.

In the case where $j \neq k$, Eq. 47 describes the spectral heat transfer to the j -th body due to thermal noise in the k -th body, i.e. $S_{k \rightarrow j}(\omega) = S_j(\omega)$. Using identity $\overline{\mathcal{Q}} = \mathcal{I} + \overline{\mathcal{T}} \overline{\mathcal{W}}$ and hence $\overline{\mathcal{Q}}_{jk} = \mathcal{T}_j \overline{\mathcal{W}}_{jk}$ when $j \neq k$, Eq. 47 can be re-written as

$$S_{k \rightarrow j}(\omega) = \frac{2}{\pi} \Theta(\omega, T_k) \text{Tr} [\mathcal{A}_j \overline{\mathcal{W}}_{jk} \mathcal{R}_k (\overline{\mathcal{W}}_{jk})^\dagger], \quad (48)$$

where

$$\mathcal{A}_j \equiv -(\mathcal{T}_j + \mathcal{T}_j^\dagger)/2 - \mathcal{T}_j^\dagger \mathcal{T}_j. \quad (49)$$

In the case where $j = k$, by negating Eq. 47, the power spectral density of the total emission out of body k is:

$$S_k^{\text{tot}}(\omega) = \frac{2}{\pi} \Theta(\omega, T_k) \text{Re} \text{Tr} [\overline{\mathcal{Q}}_{kk} \mathcal{R}_k (\overline{\mathcal{Q}}_{kk} + \overline{\mathcal{W}}_{kk})^\dagger]. \quad (50)$$

From energy balance, the energy flux out of the source body should equal the sum of the energy transfer to other bodies and the emission to the environment. Then from Eq. 50, and Eq. 47 when $j \neq k$, the emission from the source body k to the environment in the presence of other bodies is

$$S_{k \rightarrow \text{env}}(\omega) = \frac{2}{\pi} \Theta(\omega, T_k) \text{Re} \sum_{j=1}^n \text{Tr} [\overline{\mathcal{Q}}_{jk} \mathcal{R}_k (\overline{\mathcal{Q}}_{jk} + \overline{\mathcal{W}}_{jk})^\dagger], \quad (51)$$

where n is the number of bodies in the system.

Equations 47, 48, 50 and 51 are the major results of this study. They allow for evaluating heat transfer and thermal emission in reciprocal and non-reciprocal many-body systems using compact formulas. Here we briefly comment on the numerical cost for implementing these formulas. Consider the heat transfer among n bodies, and in the expansion of Eq. 45 we keep a total of N modes per body. \mathcal{T}_j and \mathcal{U}^{jl} are then $N \times N$ matrices, whereas $\overline{\mathcal{T}}, \overline{\mathcal{U}}$

and $\overline{\mathcal{W}}$ are $(Nn) \times (Nn)$ matrices. The main computation step, which is Eq. 43, involves the inversion of an $Nn \times Nn$ matrix. When using the spherical wave basis, if we specify l as the cut-off in total angular momentum included in the expansion, then $N = 2l(l+2)$.

B. Arbitrary basis

In the derivation above, we use spherical wave basis, which consists of only propagating waves. In the following, we discuss arbitrary wave basis, which generally contains propagating as well as evanescent waves. An example of such an arbitrary basis is the plane wave basis used to describe heat transfer between extended bodies, where the basis can be either propagating or evanescent depending on the magnitude of the parallel wavevectors.

The derivation above can be straightforwardly generalized with the arbitrary basis. Below we highlight the main differences. With the arbitrary wave basis, the matrix \mathcal{R} in Eq. 28 is modified as:

$$\mathcal{R} = -(\mathcal{T}e^{-i\Phi} + e^{i\Phi}\mathcal{T}^\dagger)/2 - \mathcal{T}\Pi^{pr}\mathcal{T}^\dagger. \quad (52)$$

The derivations then follow unchanged to Eq. 46. Eq. 47 is modified to:

$$S_j(\omega) = -\frac{2}{\pi}\Theta(\omega, T_k) \text{Tr Re} [\overline{\mathcal{Q}}_{jk}\mathcal{R}_k(\Pi^{pr}\overline{\mathcal{Q}}_{jk} + e^{i\Phi_j}\overline{\mathcal{W}}_{jk})^\dagger], \quad (53)$$

where $j = 1, 2, \dots, n$. In Eq. 48, the matrix \mathcal{A} is modified to:

$$\mathcal{A} = -(e^{-i\Phi}\mathcal{T} + \mathcal{T}^\dagger e^{i\Phi})/2 - \mathcal{T}^\dagger\Pi^{pr}\mathcal{T}. \quad (54)$$

Eq. 50 is modified to:

$$S_k^{tot}(\omega) = \frac{2}{\pi}\Theta(\omega, T_k)\text{Re Tr} [\overline{\mathcal{Q}}_{kk}\mathcal{R}_k(\Pi^{pr}\overline{\mathcal{Q}}_{kk} + e^{i\Phi_k}\overline{\mathcal{W}}_{kk})^\dagger]. \quad (55)$$

Eq. 51 is modified to:

$$S_{k \rightarrow env}(\omega) = \frac{2}{\pi}\Theta(\omega, T_k)\text{Re} \sum_{j=1}^n \text{Tr} [\overline{\mathcal{Q}}_{jk}\mathcal{R}_k(\Pi^{pr}\overline{\mathcal{Q}}_{jk} + e^{i\Phi_j}\overline{\mathcal{W}}_{jk})^\dagger]. \quad (56)$$

V. NUMERICAL STUDIES

A. Material properties and dielectric tensor of magneto-optical materials

We now present numerical examples of non-reciprocal near field radiative heat transfer. We consider multiple spheres with their centers lying on the $x - y$ plane. The spheres are

made of n-doped *InSb*. An external B field is applied in the z -direction to break the Lorentz reciprocity. The relative permittivity tensor of n-InSb in the presence of an external B field in the z -direction is:

$$\bar{\epsilon} = \epsilon_b \bar{I} - \frac{\omega_p^2}{(\omega + i\Gamma)^2 - \omega_c^2} \begin{bmatrix} 1 + i\frac{\Gamma}{\omega} & -i\frac{\omega_c}{\omega} & 0 \\ i\frac{\omega_c}{\omega} & 1 + i\frac{\Gamma}{\omega} & 0 \\ 0 & 0 & \frac{(\omega + i\Gamma)^2 - \omega_c^2}{\omega(\omega + i\Gamma)} \end{bmatrix}.$$

Here, the first term is the permittivity as taken from Ref. 81. This permittivity includes contributions from both interband transition and lattice vibration. The second term takes into account free-carrier contribution, which is sensitive to external magnetic field. Γ is the free carrier relaxation rate, $\omega_c = eB/m^*$ is the cyclotron frequency, and $\omega_p = \sqrt{n_e e^2 / (m^* \epsilon_0)}$ is the plasma frequency. We use a doping concentration $n_e = 1.36 \times 10^{19} \text{ cm}^{-3}$, for which the experimentally characterized relaxation rate⁸² is $\Gamma = 10^{12} \text{ s}^{-1}$ and the effective electron mass^{82,83} is $m^* = 0.08 m_e$.

We use vector spherical wave functions as the wave basis. We calculate the \mathcal{T} matrix for the sphere, by constructing the eigenmodes inside the sphere using vector spherical wave functions, and then matching the boundary conditions⁸⁴. We use a computationally-efficient recursive formalism to compute the conversion matrix \mathcal{U} using vector translation addition theorem^{79,80}.

B. Persistent heat current at thermal equilibrium

In Ref. 65, it was noted that there can be a persistent heat current in non-reciprocal many-body heat transfer. Ref. 65 considered heat transfer among three bodies. Here, as an application of the formalism presented above, we consider heat transfer for larger numbers of bodies. We show that such persistent heat current can persist for larger numbers of bodies. Moreover, the directionality of heat transfer has a non-monotonic dependency on the strength of the magnetic field.

The configuration used in our calculation is illustrated in Fig. 2a. We consider a total of n InSb spheres. Each sphere has a radius of 100 nm. The centers of the spheres are placed on the vertices of an n -sided regular polygon with a side length of 320 nm. A magnetic field is applied perpendicular to the plane of the polygon. Fig. 2a shows the case of $n = 6$.

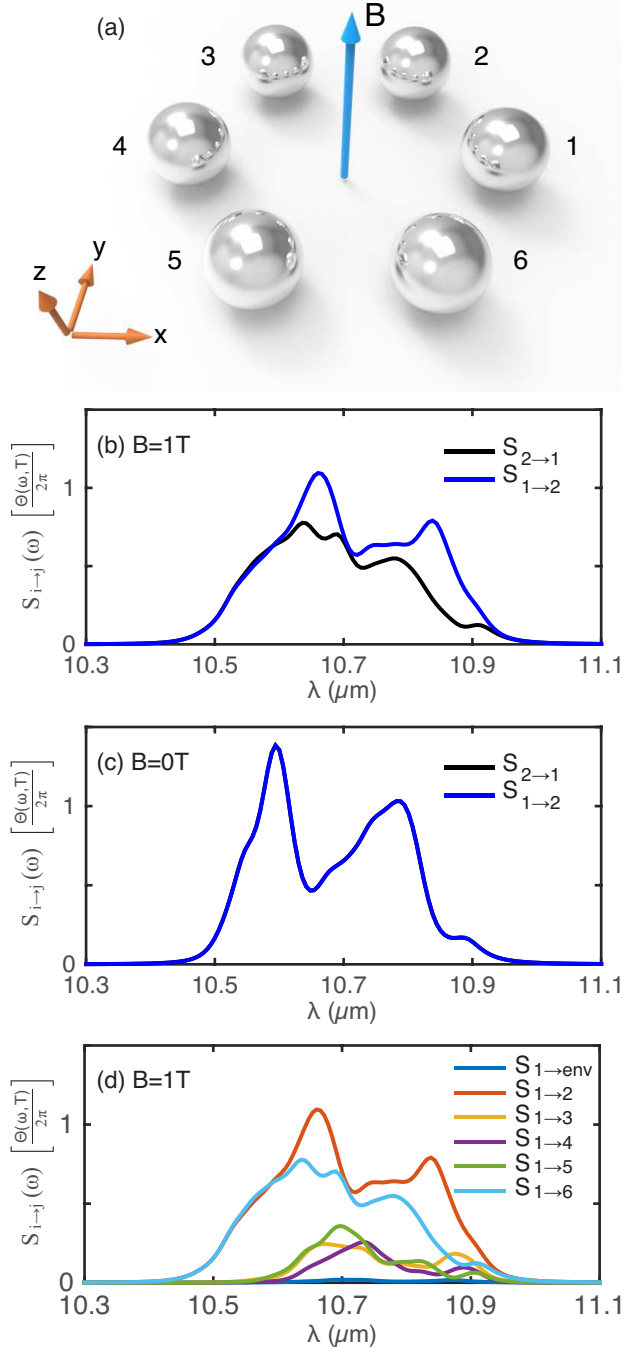


FIG. 2. (Color online) (a) Geometry of a many-body system consisting of six spheres. The centers of the spheres are placed at the vertices of a regular hexagon on x - y plane with a side length of 320 nm. Each sphere has a radius of 100 nm. A magnetic field is applied in the z direction. The spheres consist of n-doped *InSb*, with the same doping level. (b) and (c) The heat transfer spectra of $S_{2 \rightarrow 1}$ and $S_{1 \rightarrow 2}$, from fluctuational electrodynamics. The system is at equilibrium. (b) Non-reciprocal case with $B = 1\text{T}$. (c) Reciprocal case with $B = 0\text{T}$. (d) The spectra for thermal transfer from sphere 1 to other spheres and to the background environment, with $B = 1\text{T}$.

The strength of the persistent heat current between two bodies i and j can be characterized by the directionality of the heat flow between the two bodies, defined as

$$\eta_{i \rightarrow j} = (S_{i \rightarrow j} - S_{j \rightarrow i}) / \min(S_{i \rightarrow j}, S_{j \rightarrow i}).$$

For the structure shown in Fig. 2a, Fig. 2b shows the normalized heat flux spectra for $S_{2 \rightarrow 1}$ and $S_{1 \rightarrow 2}$ at the same temperature. We observe that the spectra $S_{2 \rightarrow 1}$ and $S_{1 \rightarrow 2}$ are different at $B = 1 \text{ T}$, demonstrating a directional heat flow. At the free space wavelength $\lambda = 10.88 \text{ } \mu\text{m}$, the directionality $\eta_{1 \rightarrow 2}$ is as large as 247%. After spectral integration over the entire thermal wavelength range when the temperature of the spheres are at $T = 300 \text{ K}$, the directionality for the heat transfer between bodies 1 and 2 is still as large as 32%, with $S_{1 \rightarrow 2} > S_{2 \rightarrow 1}$. In thermal equilibrium, from the rotational symmetry of the system, we then can see that there is strong persistent heat current in counter-clockwise direction. In contrast, for the scenario with $B = 0 \text{ T}$ shown in Fig. 2c, the heat transfer spectra $S_{2 \rightarrow 1} = S_{1 \rightarrow 2}$ when the spheres are at the same temperature, indicating the lack of persistent heat current.

In Fig. 2d, we plot the radiative heat transfer from body 1 to all other bodies in the structure, and also the far field radiation to the environment from body 1. We observe that the heat transfer between the spheres are much larger compared to far field radiation, indicating the near-field nature of heat transfer in this system. Also, the near field heat transfer to nearest-neighbor spheres is much larger than those to the farther spheres, in consistency with the near-field nature of the heat transfer.

The existence of the persistent heat current can be related to the nature of the electromagnetic states supported in the spheres. In the absence of external magnetic fields, an individual sphere support counter-rotating states that are degenerate to each other. In the presence of the field, the degeneracy is split, and the directionality arises from the interference effects from these states. To maximize the directionality, there is an optimum in the split of resonance frequencies, which in turn indicates the existence of an optimal external magnetic field. In Fig. 3, we study the directionality as a function of external magnetic field. And we consider structures with the number of spheres ranging from $n = 3$ to $n = 10$. In all these cases, the directionality shows a non-monotonic dependency as a function of the magnetic field strength, in consistency with the physical picture discussed above.

In general, the details of the persistent heat current show intricate dependency of both

the number of the spheres and the strength of the magnetic field. For example, at $B = 4\text{ T}$, a persistent heat current is supported in the clockwise direction in the case of $n = 3$ (blue curve, Fig. 3), whereas a persistent heat current flowing in the counter-clockwise direction can occur when $n \geq 4$. For the cases of $n = 3$ and 4, the persistent heat current can have opposite directions by varying the magnitude of the external magnetic field, while keeping the direction of the magnetic field fixed.

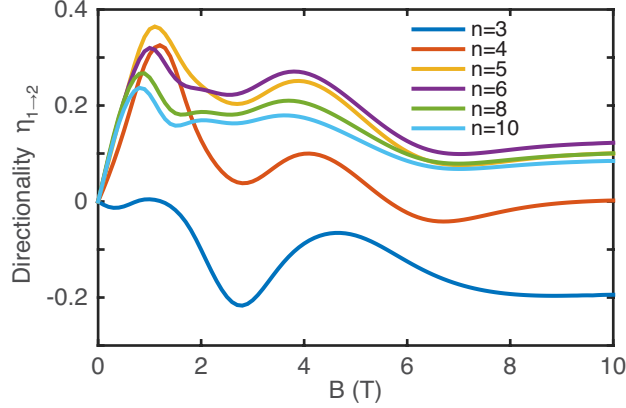


FIG. 3. (Color online) Directionality between bodies 1 and 2 as a function of external B field, in a system consisting of n InSb spheres. Each sphere has a radius of 100 nm. The centers of the spheres are placed on the vertices of n -sided regular polygon with a side length of 320 nm on x - y plane. The external magnetic field is applied in z direction. The example with $n = 6$ is shown in Fig. 2a. The system is at thermal equilibrium of 300 K.

In the examples above we have applied a magnetic field along the z -direction. Such a choice of the direction of magnetic field is important. In Fig. 4, we instead apply an external B field along the x -direction, for the case where $n = 6$. We observe that in this scenario the heat transfer is reciprocal. We have also numerically verified that for all the systems consisting of spheres forming regular polygons, applying the external B field in any direction inside the plane of the spheres always leads to reciprocal heat transfer. This observation is consistent with the discussions above relating the persistent heat current to degeneracy splitting of collective counter-rotating states. The collective rotating states reside in the plane of the spheres. Thus, in order to break the reciprocity of those states, the external magnetic field must have a non-zero out-of-plane component.

We end this section by providing some numerical details. For the case where $n = 10$, we have used a cut-off in the total angular momentum of $l_{max} = 9$. For the cases we tested,

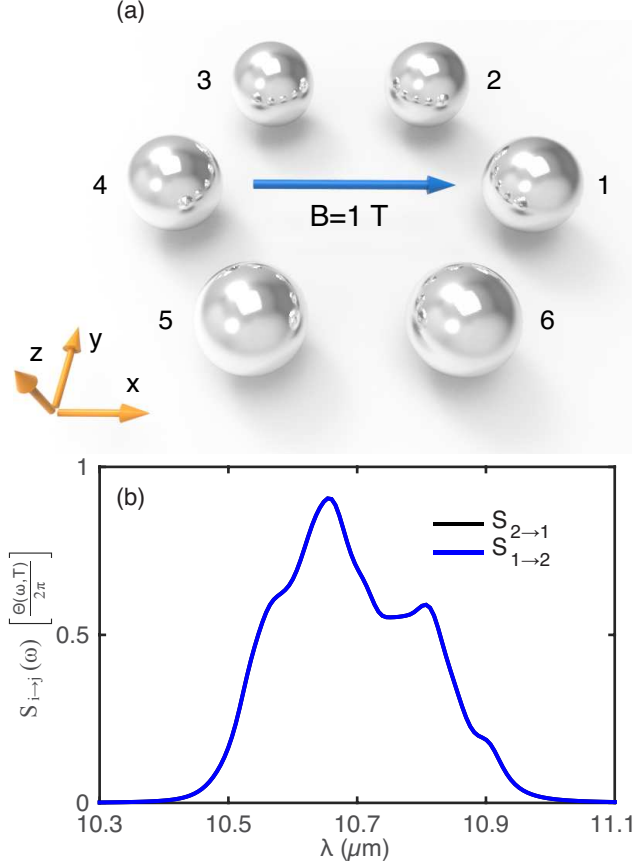


FIG. 4. (Color online) (a) Geometry of a many-body system consisting of six spheres. The centers of the spheres are placed at the vertices of a regular hexagon on x - y plane with a side length of 320 nm. Each sphere has a radius of 100 nm. An external magnetic field $B = 1$ T is applied in x direction. (b) The heat transfer spectra of $S_{2 \rightarrow 1}$ and $S_{1 \rightarrow 2}$. The system is at thermal equilibrium of 300 K.

further increasing l_{max} to 10 changes the results by a fraction that is less than 10^{-7} . For each frequency obtaining all the $S_{i \rightarrow j}$ for all instances of i and j takes about 4 seconds on a single-core machine. The results here indicate that our formalism can be used to simulate heat transfer among a substantial number of objects with relatively modest computational costs.

C. Directional heat flow at thermal non-equilibrium

The formalism as developed in Section IV is generally applicable for non-equilibrium situations where the bodies have different temperatures. In this subsection we will use this

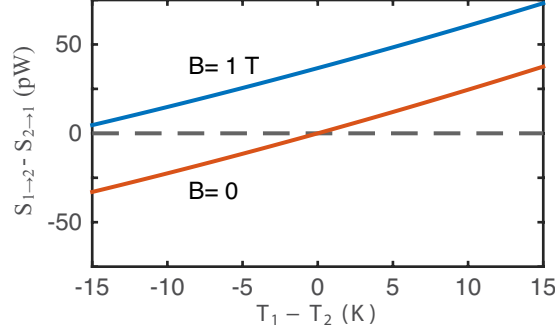


FIG. 5. (Color online) Net heat flux from body 1 to body 2. The geometry is the same as in Fig. 2a. T_2 is fixed at 300 K, while T_1 varies.

formalism to consider non-reciprocal heat transfer away from thermal equilibrium. Figure 5 shows the case where we use the same $n = 6$ geometry in Fig. 2a, but we vary the temperature T_1 of body 1 while keeping the temperature of all the other bodies fixed at 300 K. When the applied magnetic field is at $B = 1$ T, there is a directional flow from body 1 to body 2 at the equilibrium situation. Consequently, $S_{1\rightarrow 2} > S_{2\rightarrow 1}$, even when $T_1 < T_2$. We emphasize that such a result does not violate the second law of thermodynamics, since when $T_1 < T_2$, there is always a net heat flow into body 1 from the composite of all the bodies except body 1, thus the net total heat flow points from the hot to the cold, which is consistent with the second law. In contrast, with $B = 0$ T, the system is reciprocal, and $S_{1\rightarrow 2} > S_{2\rightarrow 1}$ only when $T_1 > T_2$.

The directional heat transfer as discussed above has unique signature in the dynamics of the system away from thermal equilibrium. The dynamics of the temperatures for the bodies are described by:

$$C_i \frac{d}{dt} T_i = \int_0^\infty d\omega \left\{ \sum_{j \neq i} [S_{j \rightarrow i}(\omega) - S_{i \rightarrow j}(\omega)] + S_{env \rightarrow i}(\omega) - S_{i \rightarrow env}(\omega) \right\}, \quad (57)$$

where C_i denotes the heat capacity of body i .

We consider again the case of $n = 6$ in the configuration as shown in Fig. 2a, but now studying the transient behavior of the system using Eq. 57. We maintain sphere 1 at a constant temperature of 300 K by assuming it to be in contact with a large reservoir. The other five spheres are assumed to be initially at 200 K. They are assumed to be isolated except through radiative heat contact with other spheres in the system. Consequently, due to the near field radiative heat exchange the temperatures of these five spheres will increase with

time and eventually approach 300 K . We compute the temperature as a function of time for each of the spheres using Eq. 57, where we determine C_i from the specific heat of $n - InSb$ which is 200 $J/(kg \cdot K)$. We also assume that the dielectric property of the material does not vary as a function of temperature. In Fig. 6, we show the temperatures of the spheres as a function of time. Sphere 2 which is in the counter-clockwise direction of sphere 1 is preferentially heated up, compared with sphere 6 which is the clockwise direction of sphere 1, in consistency with the existence of a persistent heat current along the counter-clockwise direction. The preferential direction for heating can be reversed by flipping the direction of the external magnetic field. On the other hand, if $B = 0$, sphere 2 and 6 will have the exact same temperature. Therefore, the persistent heat current as we predicted for the equilibrium situation can be probed in non-equilibrium experiments.

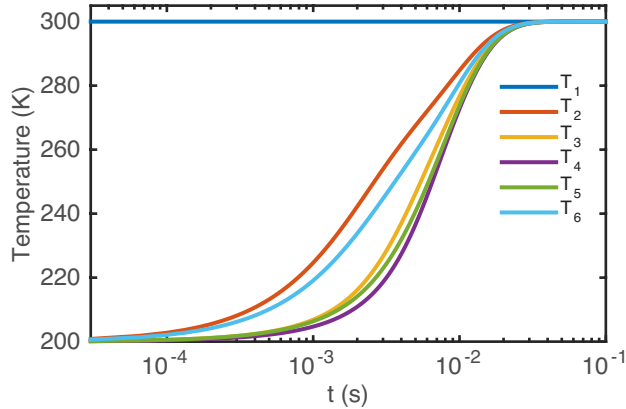


FIG. 6. (Color online) Transient behavior involving non-reciprocal many-body heat transfer in thermal non-equilibrium. The geometry parameters are the same as in Fig. 2a. An external magnetic field as $B = 1T$ is applied in z direction. Sphere 1 is fixed at 300 K , and the other spheres are initially at 200 K . Plotted here are the temperatures of all the spheres as a function of time.

VI. CONCLUSION

In summary, we have developed compact formulas to calculate near field radiative heat transfer in both reciprocal and non-reciprocal many-body systems. Such formulas allow efficient calculation of radiative heat transfer in systems consisting of a large number of particles, and take into account of all the modes. As a demonstration, we study non-

reciprocal many-body near field radiative heat transfer in and out of thermal equilibrium. In equilibrium, we show that persistent heat current has intricate dependence on the number of particles in the system and the external magnetic field. Out of thermal equilibrium, we show that non-reciprocal heat transfer points to directional heat exchange, with the direction set by the persistent heat current in equilibrium. Our work points to the opportunity of exploring novel effects of radiative heat transfer that can arise in complex reciprocal and non-reciprocal many-body systems.

ACKNOWLEDGMENTS

This work was supported by the DOE ‘Light-Material Interactions in Energy Conversion’ Energy Frontier Research Center under grant DE-SC0001293.

Appendix: Derivation of Eq. 27

Eq. 27 describes the field correlation solely due to thermal noise sources of an isolated body k . Eq. 27 has been provided in Ref. 57. For completeness, we derive it here.

We consider a single body k in thermal equilibrium with the environment. As the thermal noise sources in the body k and the environment (with infinitesimal loss) are uncorrelated, the field correlation at equilibrium can be divided according to the thermal noise sources:

$$\langle \mathbf{E}(\mathbf{r})\mathbf{E}^\dagger(\mathbf{r}') \rangle_{eq} = \langle \mathbf{E}(\mathbf{r})\mathbf{E}^\dagger(\mathbf{r}') \rangle_k^{iso} + \langle \mathbf{E}(\mathbf{r})\mathbf{E}^\dagger(\mathbf{r}') \rangle_{env},$$

where $\langle \mathbf{E}(\mathbf{r})\mathbf{E}^\dagger(\mathbf{r}') \rangle_k^{iso}$ is the contribution due to sources in the k -th body, and $\langle \mathbf{E}(\mathbf{r})\mathbf{E}^\dagger(\mathbf{r}') \rangle_{env}$ is the contribution due to sources in the environment. Thus,

$$\langle \mathbf{E}(\mathbf{r})\mathbf{E}^\dagger(\mathbf{r}') \rangle_k^{iso} = \langle \mathbf{E}(\mathbf{r})\mathbf{E}^\dagger(\mathbf{r}') \rangle_{eq} - \langle \mathbf{E}(\mathbf{r})\mathbf{E}^\dagger(\mathbf{r}') \rangle_{env}. \quad (\text{A.1})$$

On one hand, the field correlation at equilibrium is set by Eq. 18 as reproduced below:

$$\langle \mathbf{E}(\mathbf{r})\mathbf{E}^\dagger(\mathbf{r}') \rangle_{eq} = \frac{4}{\pi} \omega \Theta(\omega, T) \mu_0 \frac{\hat{G}(\mathbf{r}, \mathbf{r}') - \hat{G}^\dagger(\mathbf{r}', \mathbf{r})}{2i}. \quad (\text{A.2})$$

For the system consisting of the body k and the environment, from the Lippmann-Schwinger equation⁷³,

$$\hat{G} = \hat{G}_0 + \hat{G}_0 \hat{T}_k \hat{G}_0. \quad (\text{A.3})$$

On the other hand, $\langle \mathbf{E}(\mathbf{r})\mathbf{E}^\dagger(\mathbf{r}') \rangle_{env}$ results from the scattering by body k of the field emitted by the environment. From Eq. A.2, the field emitted by a free-space environment is described by:

$$\langle \mathbf{E}(\mathbf{r})\mathbf{E}^\dagger(\mathbf{r}') \rangle_{free} = \frac{4}{\pi}\omega\Theta(\omega, T)\mu_0 Im\hat{G}_0.$$

Using the Lippmann-Schwinger equation⁷³ and treating such free-space field \mathbf{E}^{free} as an incident field, the total field after scattering by body k is $\mathbf{E}^{env} = (1 + \hat{G}_0\hat{T}_k)\mathbf{E}^{free}$. Thus,

$$\begin{aligned}\langle \mathbf{E}(\mathbf{r})\mathbf{E}^\dagger(\mathbf{r}') \rangle_{env} &= (1 + \hat{G}_0\hat{T}_k)\langle \mathbf{E}(\mathbf{r})\mathbf{E}^\dagger(\mathbf{r}') \rangle_{free}(1 + \hat{G}_0\hat{T}_k)^\dagger, \\ &= \frac{4}{\pi}\omega\Theta(\omega, T)\mu_0 (1 + \hat{G}_0\hat{T}_k)Im\hat{G}_0(1 + \hat{G}_0\hat{T}_k)^\dagger.\end{aligned}\quad (\text{A.4})$$

Then from Eqs. A.1, A.2, A.3 and A.4, we have

$$\begin{aligned}\langle \mathbf{E}(\mathbf{r})\mathbf{E}^\dagger(\mathbf{r}') \rangle_k^{iso} &= \frac{4}{\pi}\omega\Theta(\omega, T)\mu_0 \frac{\hat{G} - \hat{G}^\dagger}{2i} - \frac{4}{\pi}\omega\Theta(\omega, T)\mu_0(1 + \hat{G}_0\hat{T}_k)Im\hat{G}_0(1 + \hat{G}_0\hat{T}_k)^\dagger, \\ &= \frac{4}{\pi}\omega\Theta(\omega, T)\mu_0 \hat{R}_k,\end{aligned}\quad (\text{A.5})$$

where

$$\hat{R}_k = \hat{G}_0 \left[\frac{\hat{T}_k - \hat{T}_k^\dagger}{2i} - \hat{T}_k Im\hat{G}_0\hat{T}_k^\dagger \right] \hat{G}_0^\dagger.$$

Further, by using Eqs. 14, 15 and 16, we have

$$\langle \mathbf{E}(\mathbf{r})\mathbf{E}^\dagger(\mathbf{r}') \rangle_k^{iso} = \frac{4}{\pi}\omega\Theta(\omega, T)\mu_0 \sum_{\nu, \nu'} \mathbf{E}_{k, \nu}^{out}(\mathbf{r}) (\mathcal{R}_k)_{\nu, \nu'} \mathbf{E}_{k, \nu'}^{out\dagger}(\mathbf{r}'), \quad (\text{A.6})$$

where in spherical wave basis

$$\mathcal{R}_k = -(\mathcal{T}_k + \mathcal{T}_k^\dagger)/2 - \mathcal{T}_k \mathcal{T}_k^\dagger.$$

* linxiao.zhu.lx.zhu@gmail.com

† shanhui@stanford.edu

¹ D. Polder and M. Van Hove, Phys. Rev. B **4**, 3303 (1971).

² J. J. Loomis and H. J. Maris, Phys. Rev. B **50**, 18517 (1994).

³ J. Pendry, J. Phys. Condens. Matter **11**, 6621 (1999).

⁴ A. V. Shchegrov, K. Joulain, R. Carminati, and J.-J. Greffet, Phys. Rev. Lett. **85**, 1548 (2000).

- ⁵ V. Chiloyan, J. Garg, K. Esfarjani, and G. Chen, *Nat. Commun.* **6**, 6755 (2015).
- ⁶ S. Shen, A. Narayanaswamy, and G. Chen, *Nano Lett.* **9**, 2909 (2009).
- ⁷ E. Rousseau, A. Siria, G. Jourdan, S. Volz, F. Comin, J. Chevrier, and J.-J. Greffet, *Nat. Photonics* **3**, 514 (2009).
- ⁸ T. Kralik, P. Hanzelka, M. Zobac, V. Musilova, T. Fort, and M. Horak, *Phys. Rev. Lett.* **109**, 224302 (2012).
- ⁹ R. St-Gelais, B. Guha, L. Zhu, S. Fan, and M. Lipson, *Nano Lett.* **14**, 6971 (2014).
- ¹⁰ K. Kim, B. Song, V. Fernández-Hurtado, W. Lee, W. Jeong, L. Cui, D. Thompson, J. Feist, M. T. H. Reid, F. J. García-Vidal, J. C. Cuevas, E. Meyhofer, and P. Reddy, *Nature* **528**, 387 (2015).
- ¹¹ B. Song, Y. Ganjeh, S. Sadat, D. Thompson, A. Fiorino, V. Fernández-Hurtado, J. Feist, F. J. Garcia-Vidal, J. C. Cuevas, P. Reddy, and E. Meyhofer, *Nature Nanotechnol.* **10**, 253 (2015).
- ¹² R. St-gelais, L. Zhu, S. Fan, and M. Lipson, *Nature Nanotechnol.* **11**, 515 (2016).
- ¹³ B. Song, D. Thompson, A. Fiorino, Y. Ganjeh, P. Reddy, and E. Meyhofer, *Nature Nanotechnol.* **11**, 509 (2016).
- ¹⁴ M. P. Bernardi, D. Milovich, and M. Francoeur, *Nat. Commun.* **7**, 12900 (2016).
- ¹⁵ J. I. Watjen, B. Zhao, and Z. M. Zhang, *Appl. Phys. Lett.* **109**, 203112 (2016).
- ¹⁶ L. Cui, W. Jeong, V. Fernández-Hurtado, J. Feist, F. J. García-Vidal, J. C. Cuevas, E. Meyhofer, and P. Reddy, *Nat. Commun.* **8**, 14479 (2017).
- ¹⁷ K. Kloppstech, N. Könné, S.-A. Biehs, A. W. Rodriguez, L. Worbes, D. Hellmann, and A. Kittel, *Nat. Commun.* **8**, 14475 (2017).
- ¹⁸ A. Kittel, W. Müller-Hirsch, J. Parisi, S.-A. Biehs, D. Reddig, and M. Holthaus, *Phys. Rev. Lett.* **95**, 224301 (2005).
- ¹⁹ Y. De Wilde, F. Formanek, R. Carminati, B. Gralak, P.-A. Lemoine, K. Joulain, J.-P. Mulet, Y. Chen, and J.-J. Greffet, *Nature* **444**, 740 (2006).
- ²⁰ A. Narayanaswamy and G. Chen, *Appl. Phys. Lett.* **82**, 3544 (2003).
- ²¹ S. Molesky and Z. Jacob, *Phys. Rev. B* **91**, 205435 (2015).
- ²² M. Laroche, R. Carminati, and J.-J. Greffet, *J. Appl. Phys.* **100**, 063704 (2006).
- ²³ S. Basu, Y.-B. Chen, and Z. M. Zhang, *Int. J. Energy Res.* **31**, 689 (2007).
- ²⁴ K. Park, S. Basu, W. King, and Z. Zhang, *J. Quant. Spectrosc. Radiat. Transfer* **109**, 305 (2008).

- ²⁵ S. Basu, Z. M. Zhang, and C. J. Fu, *Int. J. Energy Res.* **33**, 1203 (2009).
- ²⁶ K. Chen, P. Santhanam, and S. Fan, *Appl. Phys. Lett.* **107**, 091106 (2015).
- ²⁷ K. Chen, P. Santhanam, S. Sandhu, L. Zhu, and S. Fan, *Phys. Rev. B* **91**, 134301 (2015).
- ²⁸ X. Liu and Z. M. Zhang, *Nano Energy* **26**, 353 (2016).
- ²⁹ C. R. Otey, W. T. Lau, and S. Fan, *Phys. Rev. Lett.* **104**, 154301 (2010).
- ³⁰ S. Basu and M. Francoeur, *Appl. Phys. Lett.* **98**, 113106 (2011).
- ³¹ H. Iizuka and S. Fan, *J. Appl. Phys.* **112**, 024304 (2012).
- ³² L. Zhu, C. R. Otey, and S. Fan, *Phys. Rev. B* **88**, 184301 (2013).
- ³³ L. P. Wang and Z. M. Zhang, *Nanoscale Microsc. Therm.* **17**, 337 (2013).
- ³⁴ Y. Yang, S. Basu, and L. Wang, *Appl. Phys. Lett.* **103**, 163101 (2013).
- ³⁵ P. Ben-Abdallah and S.-A. Biehs, *Phys. Rev. Lett.* **112**, 044301 (2014).
- ³⁶ A. W. Rodriguez, O. Ilic, P. Bermel, I. Celanovic, J. D. Joannopoulos, M. Soljačić, and S. G. Johnson, *Phys. Rev. Lett.* **107**, 114302 (2011).
- ³⁷ R. Guerout, J. Lussange, F. S. S. Rosa, J.-P. Hugonin, D. A. R. Dalvit, J.-J. Greffet, A. Lambrecht, and S. Reynaud, *Phys. Rev. B* **85**, 180301 (2012).
- ³⁸ J. Lussange, R. Guérout, F. S. S. Rosa, J. J. Greffet, A. Lambrecht, and S. Reynaud, *Phys. Rev. B* **86**, 085432 (2012).
- ³⁹ X. Liu and Z. Zhang, *ACS Photonics* **2**, 1320 (2015).
- ⁴⁰ X. Liu, B. Zhao, and Z. M. Zhang, *Phys. Rev. A* **91**, 062510 (2015).
- ⁴¹ J. Dai, S. A. Dyakov, and M. Yan, *Phys. Rev. B* **92**, 035419 (2015).
- ⁴² H. Chalabi, E. Hasman, and M. L. Brongersma, *Phys. Rev. B* **91**, 014302 (2015).
- ⁴³ H. Chalabi, E. Hasman, and M. L. Brongersma, *Phys. Rev. B* **91**, 174304 (2015).
- ⁴⁴ J. Dai, S. A. Dyakov, S. I. Bozhevolnyi, and M. Yan, *Phys. Rev. B* **94**, 125431 (2016).
- ⁴⁵ J. Dai, S. A. Dyakov, and M. Yan, *Phys. Rev. B* **93**, 155403 (2016).
- ⁴⁶ R. Messina, A. Noto, B. Guizal, and M. Antezza, *Phys. Rev. B* **95**, 125404 (2017).
- ⁴⁷ V. Fernández-Hurtado, F. J. García-Vidal, S. Fan, and J. C. Cuevas, *Phys. Rev. Lett.* **118**, 203901 (2017).
- ⁴⁸ S.-A. Biehs, M. Tschikin, and P. Ben-Abdallah, *Phys. Rev. Lett.* **109**, 104301 (2012).
- ⁴⁹ Y. Guo, C. L. Cortes, S. Molesky, and Z. Jacob, *Appl. Phys. Lett.* **101**, 131106 (2012).
- ⁵⁰ Y. Guo and Z. Jacob, *Opt. Exp.* **21**, 15014 (2013).
- ⁵¹ J. Shi, B. Liu, P. Li, L. Y. Ng, and S. Shen, *Nano Lett.* **15**, 1217 (2015).

- ⁵² M. Francoeur, M. P. Meng, and R. Vaillon, Appl. Phys. Lett. **93**, 043109 (2008).
- ⁵³ O. D. Miller, S. G. Johnson, and A. W. Rodriguez, Phys. Rev. Lett. **112**, 157402 (2014).
- ⁵⁴ A. Narayanaswamy and G. Chen, Phys. Rev. B **77**, 075125 (2008).
- ⁵⁵ R. Messina and M. Antezza, Phys. Rev. A **84**, 042102 (2011).
- ⁵⁶ C. Otey and S. Fan, Phys. Rev. B **84**, 245431 (2011).
- ⁵⁷ M. Krüger, G. Bimonte, T. Emig, and M. Kardar, Phys. Rev. B **86**, 115423 (2012).
- ⁵⁸ R. Messina, M. Antezza, and P. Ben-Abdallah, Phys. Rev. Lett. **109**, 244302 (2012).
- ⁵⁹ A. W. Rodriguez, M. T. H. Reid, J. Varela, J. D. Joannopoulos, F. Capasso, and S. G. Johnson, Phys. Rev. Lett. **110**, 014301 (2013).
- ⁶⁰ E. Moncada-Villa, V. Fernández-Hurtado, F. J. García-Vidal, A. García-Martín, and J. C. Cuevas, Phys. Rev. B **92**, 125418 (2015).
- ⁶¹ R. M. Abraham Ekeröth, A. García-Martín, and J. C. Cuevas, Phys. Rev. B **95**, 235428 (2017).
- ⁶² B. Müller, R. Incardone, M. Antezza, T. Emig, and M. Krüger, Phys. Rev. B **95**, 085413 (2017).
- ⁶³ D. Jalas, A. Petrov, M. Eich, W. Freude, S. Fan, Z. Yu, R. Baets, M. Popović, A. Melloni, J. D. Joannopoulos, M. Vanwolleghem, C. R. Doerr, and H. Renner, Nat. Photonics **7**, 579 (2013).
- ⁶⁴ P. Ben-Abdallah, Phys. Rev. Lett. **116**, 084301 (2016).
- ⁶⁵ L. Zhu and S. Fan, Phys. Rev. Lett. **117**, 134303 (2016).
- ⁶⁶ P. Ben-Abdallah, S.-A. Biehs, and K. Joulain, Phys. Rev. Lett. **107**, 114301 (2011).
- ⁶⁷ R. Messina, M. Tschikin, S.-A. Biehs, and P. Ben-Abdallah, Phys. Rev. B **88**, 104307 (2013).
- ⁶⁸ P. Ben-Abdallah, R. Messina, S.-A. Biehs, M. Tschikin, K. Joulain, and C. Henkel, Phys. Rev. Lett. **111**, 174301 (2013).
- ⁶⁹ I. Latella and P. Ben-Abdallah, Phys. Rev. Lett. **118**, 173902 (2017).
- ⁷⁰ C. R. Otey, L. Zhu, S. Sandhu, and S. Fan, J. Quant. Spectrosc. Radiat. Transfer **132**, 3 (2014).
- ⁷¹ A. G. Polimeridis, M. T. H. Reid, W. Jin, S. G. Johnson, J. K. White, and A. W. Rodriguez, Phys. Rev. B **92**, 134202 (2015).
- ⁷² W. Jin, A. G. Polimeridis, and A. W. Rodriguez, Phys. Rev. B **93**, 121403 (2016).
- ⁷³ B. Lippmann and J. Schwinger, Phys. Rev. **337**, 469 (1950).
- ⁷⁴ V. A. Golyk, M. Krüger, and M. Kardar, Phys. Rev. E **85**, 046603 (2012).
- ⁷⁵ G. S. Agarwal, Phys. Rev. A **11**, 230 (1975).
- ⁷⁶ L. Landau, E. Lifshitz, and L. Pitaevskii, *Course of Theoretical Physics Vol. 9, Statistical Physics Part 2* (Pergamon, 1980) Chap. VIII, Electromagnetic Fluctuations, p. 319.

- ⁷⁷ W. Eckhardt, Phys. Rev. A **29**, 1991 (1984).
- ⁷⁸ S. J. Rahi, T. Emig, N. Graham, R. L. Jaffe, and M. Kardar, Phys. Rev. D **80**, 085021 (2009).
- ⁷⁹ W. Chew, J. Electromagnet. Wave **6**, 133 (1992).
- ⁸⁰ W. Chew and Y. Wang, J. Electromagnet. Wave **7**, 651 (1993).
- ⁸¹ E. Palik, *Handbook of Optical Constants of Solids, Vols I, II, and III* (Elsevier Science & Tech: New York, 1985).
- ⁸² S. Law, R. Liu, and D. Wasserman, J. Vac. Sci. Technol. B **32**, 052601 (2014).
- ⁸³ P. Byszewski, J. Kolodziejczak, and S. Zukotynski, Phys. Status Solidi B **3**, 1880 (1963).
- ⁸⁴ J. L. W. Li and W. L. Ong, IEEE Trans. Antennas Propag. **59**, 3370 (2011).